Received: 27 July 2018 | Revised: 12 April 2019 | Accepted: 14 May 2019

DOI: 10.1002/joc.6164

RESEARCH ARTICLE

International Journal of Climatology RMetS

Space–time variability of drought over Vietnam

Phong V. V. Le[1] | **Tan Phan-Van**[1] | **Khiem V. Mai**[2] | **Duc Q. Tran**[1]

[1]Faculty of Hydro-Meteorology and Oceanography, VNU University of Science, Hanoi, Vietnam

[2]Vietnam Institute of Meteorology, Hydrology and Climate Change, Hanoi, Vietnam

Correspondence
Tan Phan-Van, Faculty of Hydrology Meteorology and Oceanography, VNU University of Science, 334 Nguyen Trai, Thanh Xuan, Hanoi, Vietnam.
Email: phanvantan@hus.edu.vn

Funding information
National Foundation for Science and Technology Development, Grant/Award Number: 105.06-2017.320; National Project, Grant/Award Number: KC.09.15/16-20

Abstract

Drought may have severe societal, economic, and environmental consequences. However, the space–time characteristics of drought over Vietnam remain poorly understood. In this study, we investigate the spatio-temporal variability of drought using the Palmer Drought Severity Index (PDSI) over mainland Vietnam for the 1980–2014 period. Through data analysis at 131 stations, we identified the main characteristics, historical trends, and dominant variability of drought across seven climatic sub-regions in Vietnam. The results show regional patterns of drought duration, inter-arrival time, frequency, and severity, but no consistent trend of drought variation during the study period. Based on the supply and demand concepts of water balance, PDSI captures well the large frequency and severity of drought in some sub-regions that are related to soil moisture deficit associated with high temperature and low rainfall during summer. Moreover, drought over Vietnam was predominantly controlled by climate seasonality. The linkages between drought in Vietnam and large-scale drivers are quite different among areas, suggesting a possibility of early prediction for drought at some sub-regions using ENSO.

KEYWORDS

drought, ENSO, variability, Vietnam

1 | INTRODUCTION

Drought is a fundamental and recurring extreme climate event over terrestrial land that often causes immense damage to agriculture, environment, and societies (WMO, 2006). It remains the costliest and major natural disaster which affects a very large number of people across the globe every year (Wilhite, 2000). Unlike other natural hazards (i.e., flood, storms, earthquakes, tornadoes, etc.), drought events often develop slowly and unnoticed and have diverse consequences on terrestrial ecosystems (Van Loon, 2015). Drought is generally classified into four types: meteorological, soil moisture or agricultural, hydrological, and socioeconomic droughts (Wilhite and Glantz, 1985; AMS, 2004; Mishra and Singh, 2010). Among these types, meteorological drought is the most prevalent and important since it often acts as the starting points of the others. Meteorological drought is identified by precipitation deficits, possibly combined with increased potential evapotranspiration (ET), over a region for a period of time (WMO, 2006). It can last for a wide range of temporal scales and its spatial extent is usually larger than that of other natural hazards. As a result, meteorological drought may vary significantly from one region to another due to the heterogeneity in the landscape and climatic conditions.

Drought events are often characterized by multiple characteristics (Dracup *et al.,* 1980; Ge *et al.,* 2016), including duration, inter-arrival time, peak intensity, frequency, and severity. Each of these characteristics may impact environment in very different ways. For instance, severe droughts, even in short durations, would have a catastrophic impact on agriculture during the growth stages of the crops (Rippey, 2015). In contrast, mild and moderate droughts with long durations would have devastating consequences on ecosystems and water supply (AghaKouchak, 2015). Moreover, the

variability of the inter-arrival time also affects the resilience and recovery of ecosystems under drought conditions (Schwalm *et al.,* 2017).

Given a heavy dependence on the frequency, intensity, and timing of drought for sustainable agriculture and water resources management, changes in these characteristics could pose serious threats on economics, ecology, and society. Much research has thus been made in documenting the observed changes in drought characteristics over Vietnam (Tran, 2012; Vu-Thanh *et al.,* 2014; Vu *et al.,* 2015; Le *et al.,* 2016; Vu and Mishra, 2016; Vu *et al.,* 2017). Nevertheless, most of these studies have primarily focused on rainfall variability (i.e., the Standardized Precipitation Index—SPI) or both rainfall and temperature (i.e., the Peday's index - PED, de Martonne index—J, and Standardized Precipitation Evapotranspiration Index—SPEI), and little is known about the effects of soil water balance on drought and how their combinations with evapotranspiration (ET) exacerbate the impacts of drought events. In fact, the state of soil moisture signifying water deficit is controlled by not only precipitation deficit but also excess ET (Lima and AghaKouchak, 2017). In addition, previous studies have shown that univariate risk assessment methods using rainfall only may underestimate the risk of extreme drought events (AghaKouchak *et al.,* 2014; Shukla *et al.,* 2015). In this sense, a multivariate approach such as the Palmer Drought Severity Index (PDSI; see Palmer (1965)) is therefore necessary to provide a more realistic assessment, especially under the context of global warming.

The PDSI and its self-calibrating variants are among the most prominent indices of meteorological drought and have been pervasively used to make quantification of drought's severity globally (Dai *et al.,* 2004; Sheffield *et al.,* 2012) and across different climates (Lloyd-Hughes and Saunders, 2002; Xukai *et al.,* 2005; van der Schrier *et al.,* 2006; Ge *et al.,* 2016; Li *et al.,* 2017; Lima and AghaKouchak, 2017). Unlike many other drought indices that are purely based on rainfall, PDSI is constructed based upon a primitive and simple bucket water balance model. It is calculated by integrating rainfall, temperature and soil-water holding capacity to estimate a local water balance and define moisture stress (Wells *et al.,* 2004). The PDSI is thus capable of capturing the effect of surface warming on drought that has occurred since the 20th century. Because PDSI is normalized on the basis of local average moisture conditions, it facilitates the quantitative comparison of drought incidence across different times and locations (Cook *et al.,* 2015) and is able to capture extreme events at frequencies expected for rare conditions.

Characterizing the variability and trends of drought is of primary importance for developing appropriate drought mitigation strategies. This characterization is often based on multiple drought characteristics (Dracup *et al.,* 1980; Zargar *et al.,* 2011; Saghafian and Mehdikhani, 2014; Ge *et al.,* 2016). Nevertheless, most of drought studies in Vietnam have only focused on the probability and frequency of drought occurrence, and none has addressed other important characteristics of drought events. This study attempts to bring out comprehensive aspects and valid evidences of drought across Vietnam. Here, we aim to develop understanding and analyse the trends of drought characteristics in the mainland Vietnam using PDSI. Specifically, we identify continuous changes in the space–time variation patterns of drought events across Vietnam during the 1980–2014 period. We next employ a multivariate approach for extracting the dominant variability of drought in the study area. Then, the relationships between occurrences of drought and large-scale circulation characteristics are analysed. Our hypothesis is that precipitation and temperature in Vietnam that control the variability of drought patterns are influenced by both local climate seasonality and large-scale drivers. This study for the first time presents the spatio-temporal dynamics of droughts in Vietnam as informed by the PDSI. The rest of the paper is organized as follows. In the next section, we describe the methods and datasets used in this study, followed by a description of drought indices and characteristics. The space–time variability patterns and changes of droughts are then presented in Section 3. In this section, we discuss seasonal and interannual variability, regional patterns, and trends of PDSI and its linkages with large-scale drivers. Finally, a summary is given in Section 4.

2 | MATERIALS AND METHODS

2.1 | Study area

We performed the study for the entire mainland Vietnam. Located along the east coast of the Indochina peninsula (8°–23°N and 102°−110°E), mainland Vietnam is in the intertropical zone of the Northern Hemisphere, having a long coastline of more than 3,000 km (Figure 1). It has a tropical climate modulated by the Asian monsoon systems: (i) the northeasterly monsoon in the winter (November–April) and (ii) the southwesterly monsoon in the summer (May–October), in which April–May and October–November are the transitional months between the seasons. There are two primary high mountain ranges whose directions that are almost orthogonal to the prevailing wind, namely Hoang Lien Son in the north and Truong Son along the west border of Vietnam, respectively. The spatial classification of climate in Vietnam is complicated as a result of monsoon influence, heterogeneous topography, and latitudinal extent. For this reason, the climate of Vietnam is divided into seven sub-regions as usual for analyses (Phan *et al.,* 2009; Mai *et al.,* 2014; Vu-Thanh *et al.,* 2014): Northwest (R1), Northeast (R2), Red River Delta (R3), North Central (R4), South Central (R5), Central High- land (R6), and Southern (R7).

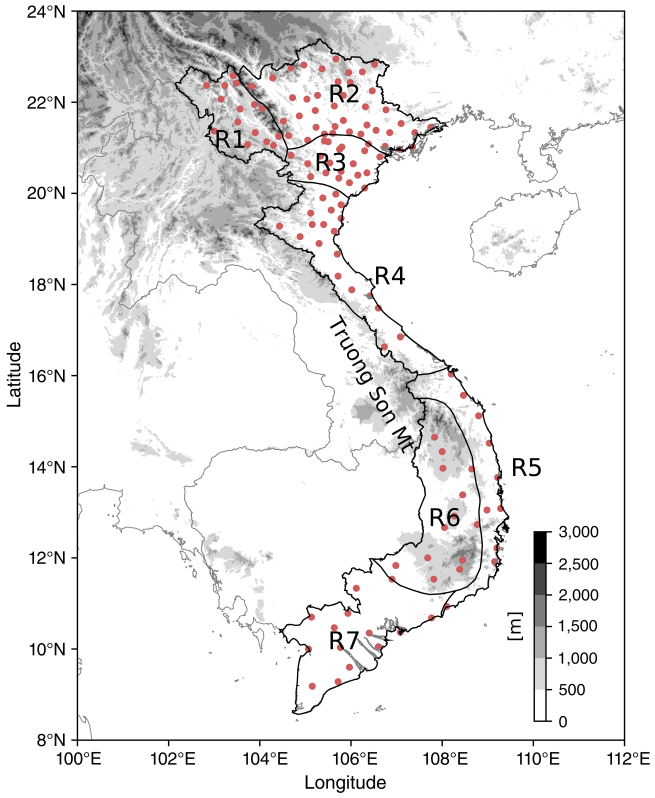

FIGURE 1 Maps of climatic sub-regions in Vietnam and 131 meteorological stations used in this study [Colour figure can be viewed at wileyonlinelibrary.com]

2.2 | Drought index

We used the well-known PDSI (Palmer, 1965) to investigate drought conditions. The classification of PDSI drought severity is presented in Table 1. Here, we considered two combined categories of PDSI for analyses:

$$C_j := \bigcup_{i=j}^{4} D_i : j = \{2,3\}, \quad (1)$$

in which D_i represents the severity of the Palmer classification. Note that, by definition, $C_3 \subseteq C_2$. Readers are referred to previous studies for the mathematical foundations of PDSI and its self-calibrating variants (Palmer, 1965; Alley, 1984; Karl, 1986; Wells *et al.,* 2004; Dai, 2010). The Thornthwaite method (Thornthwaite and Mather, 1955) is used to estimate PET for calculation of PDSI.

TABLE 1 Palmer classification of drought severity

Drought severity	Intervals	Classification	
Incipient dry	$-1 \le$ PDSI < -0.5	D_o	
Mild drought	$-2 \le$ PDSI < -1	D_1	
Moderate drought	$-3 \le$ PDSI < -2	D_2	C_2
Severe drought	$-4 \le$ PDSI < -3	D_3	C_2
Extreme drought	PDSI < -4	D_4	C_3

2.3 | Data

Observations of climatic variables and soil water-holding capacity data were used as input for the calculation of PDSI. Particularly, climatic datasets consisted of monthly precipitation and 2-m air temperature observations for the period 1980–2014 obtained from 131 meteorological stations across mainland Vietnam (see Figure 1). The study is limited to this period because long-term meteorologically based datasets are lacking in southern Vietnam (R5-R7) before 1980. These datasets were collected and provided by the Vietnam Meteorological and Hydrological Administration (http://kttvqg.gov.vn/). Soil data used for water balance and PDSI calculations included the global gridded (32×32 km) soil available water capacity (AWC), also known as field capacity. It has been shown that PDSI is sensitive to both AWC and ET (Alley, 1984; van der Schrier *et al.,* 2006). Here, AWC data were obtained from and validated using the Harmonized World Soil Database (FAO/IIASA/ISRIC/ISS-CAS/JRC, 2009).

2.4 | Drought characteristics

In this study, drought events and characteristics at all stations were identified using calculated monthly PDSI for the total period of 35 years (1980–2014). Specifically, a drought event in category C_j shown in (1) is defined as the period in which PDSI is continuously below a critical threshold Ω_j. Here, $\Omega_2 = -2$ and $\Omega_3 = -3$ for C_2 and C_3, respectively. For each category, we identified and analysed the following four main drought characteristics (see Figure 2): duration (D_u), frequency (F), inter-arrival time (T), and severity (S).

- Duration D_u of a drought event in a category C_j is identified as the number of consecutive months in which the drought index PDSI is below Ω_j.
- Inter-arrival time T of droughts is the duration (month) between the initiation time of two successive drought events (regardless of the length) in the same drought category C_j. It includes the drought and subsequent non-drought periods. Therefore, T characterizes the timing variability of drought events.
- Frequency F of droughts in category C_j over a period of time N (months) is the probability of occurring drought, calculated as the ratio of total drought duration and the total time N:

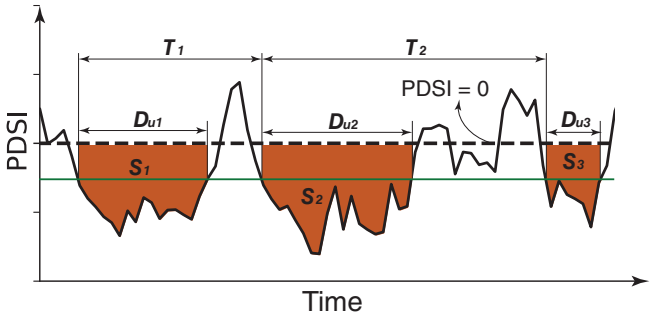

FIGURE 2 Illustration of drought events and characteristics. Du is duration, T is inter-arrival time, and S is severity [Colour figure can be viewed at wileyonlinelibrary.com]

$$F_j = \frac{\sum_{i=1}^{m} Du_i}{N} 100\%, \quad (2)$$

where m is the number of drought events in C_j.

- Severity S of a drought event in the category C_j is the cumulative PDSI drought index during the event:

$$S_j = \sum_{k=1}^{Du} PDSI_k \mid PDSI_k < \Omega_j \quad (3)$$

in which $j := \{2, 3\}$.

2.5 | Climate indices

Seasonal variations of drought events in Vietnam are also influenced by large-scale atmospheric and ocean processes. While ENSO events do not have a clear effect on drought in the northern sub-regions, drought (wetness) conditions have been observed in the southern sub-regions during El Niño (La Niña) year (Vu-Thanh *et al.,* 2014; Vu *et al.,* 2015). In order to quantify the control of large-scale climate-driven factors on drought characteristics, the correlations between calculated PDSI and 16 selected climate indices (hereafter referred to as CIs, see Table 2) reflecting the oscillatory behaviours of climate variability at different time scales were analysed. We refer the reader to the websites (ESRL-PSD, 2018; CPC, 2011) for the detailed descriptions and temporal data of these climate indices.

2.6 | Trend analysis methods

Tests for the detection of significant trends in time series data can be classified as parametric and non-parametric methods. While parametric trend tests require data to be independent and normally distributed, non-parametric trend tests only require that the data be independent (Gocic and Trajkovic, 2014). In order to examine the trends of drought index, we first used the non-parametric Mann-Kendall (Mann, 1945; Kendall, 1955) test at 5% significance level to determine the existence of monotonic trends for the variation of PDSI. Then, the Sen's slope estimator (Sen, 1968) is used to determine the magnitude of detected trends.

TABLE 2 List of 16 climate indices

ID	Index	Description and data source
1	ONI	Oceanic Niño Index
2	SOI	Southern Oscillation Index
3	Nino3.4	East Central Tropical Pacific SST
4	MEI	Multivariate ENSO Index
5	RINDO_SLPA	Equatorial SOI Indonesia SLP (Standardized Anomalies)
6	CPAC850	850 mb Trade Wind Index Central Pacific
7	REQSOI	Equatorial SOI (Standardized Anomalies)
8	WPC850	850 mb Trade Wind Index West Pacific
9	BEST	Bivariate ENSO Time Series
10	PDO	Pacific Decadal Oscillation
11	DMI	Dipole Mode Index
12	TNI	Trans-Niño Index
13	PNA	Pacific North American Index
14	WHWP	Western Hemisphere Warm Pool
15	WP	Western Pacific Index
16	QBO	Quasi-Biennial Oscillation

2.7 | Principle component analysis

It is difficult to directly analyse the spatial and temporal characteristics of the PDSI dataset at all stations. A necessary step is to reduce the dimensionality of this dataset to as few modes as possible. Here, the dominant variability of drought was extracted using a Principle Component Analysis (PCA, see (Abdi and Williams, 2010)) to the calculated monthly PDSI over 131 stations. PCA is often used for reducing data dimensionality while retaining dominant trends and patterns. We briefly summarize PCA as follow.

Given a dataset of n observations of m variables $\mathbf{x_1}$, ..., $\mathbf{x_m}$ or, equivalently, an $n \times m$ matrix $\mathbf{X}$. PCA reduces $\mathbf{X}$ by geometrically projecting it onto lower dimensions called principal components (PCs), with the goal of finding the best summary of $\mathbf{X}$ using a limited number k of PCs (Ringnér, 2008; Lever *et al.,* 2017). $\mathbf{X}$ can be written as a random function of $X(t,s)$ as:

$$X(t,s) = \sum_{i=1}^{n} EOF_i(t).PC_i(s)$$

$$\approx \sum_{i=1}^{k} EOF_i(t).PC_i(s), \quad k \ll n, \quad (4)$$

where all k vectors EOF_i are orthogonal to each other and $PC_i^T \times PC_i$ equals the i^{th} eigenvalue.

3 | RESULTS AND DISCUSSION

3.1 | Seasonal variability of temperature and precipitation

The characteristics of climate in Vietnam are influenced by the annual variations in the atmospheric circulation over Southeast Asia. Figure 3 shows the annual cycles of the mean air temperature and rainfall for the 1980–2014 period over seven climatic sub-regions. The results first indicated strong and consistent seasonal variations of both air temperature and rainfall in the northern sub-regions (R1-R3) with the maximum and minimum values occurring during summer (JJA) and winter (DJF) time, respectively. Air temperature in R1 was lowest as a result of high topographic elevation compared to R2-R3. Second, similar patterns of seasonal air temperature to R1-R3, with larger mean values, were observed in the central sub-regions (R4-R5). Nevertheless, there were timing and magnitude differences in the seasonality of rainfall between the north and central sub-regions. Unlike R1-R3, rainy seasons in R4-R5 occurred in autumn (SON), accounting for 75–90% of the annual rainfall. Note that the higher mean monthly air temperature associated with narrow, steep hill slope topography in the central sub-regions may significantly reduce the residence time of overland and stream flow. Consequently, soil moisture deficit during spring and summer time in this area was expected. Finally, seasonal variations of air temperature and rainfall were much smaller in the Central Highland (R6) and Southern (R7) sub-regions than others. Similar to R1, the larger topographic elevation in R6 resulted in a lower mean air temperature than in R7. While the mean monthly air temperature in R7 was consistently high throughout the year, rainfall during late winter time (JFM) was very low, suggesting that moisture deficit likely happens during the dry season in this area as well.

3.2 | Seasonal variability of drought

Drought is often associated with seasonality in climate. To examine the variability of drought events, we first computed monthly PDSI at all stations and then estimated the annual cycles of the key drought characteristics. The temporal variability of sub-regional means of drought frequency F, severity S, and spatial extent SE for all sub-regions are shown in Figure 4. The plots generally show an in-phase relation over most sub-regions, signifying a closed correlation between these characteristics. Much larger values of F, $|S|$, and SE for both C_2 and C_3 categories were found in R5 compared to other sub-regions. The largest values of these characteristics were observed in late spring and early summer time (AMJ). This is to be expected, due to soil moisture deficit resulting from the combined effects of high air temperature and very low amount of rainfall during this period. In contrast, F, $|S|$, and SE in R1 were smallest as a result of low mean air temperature and the timing of seasonal rainfall. Interestingly, the

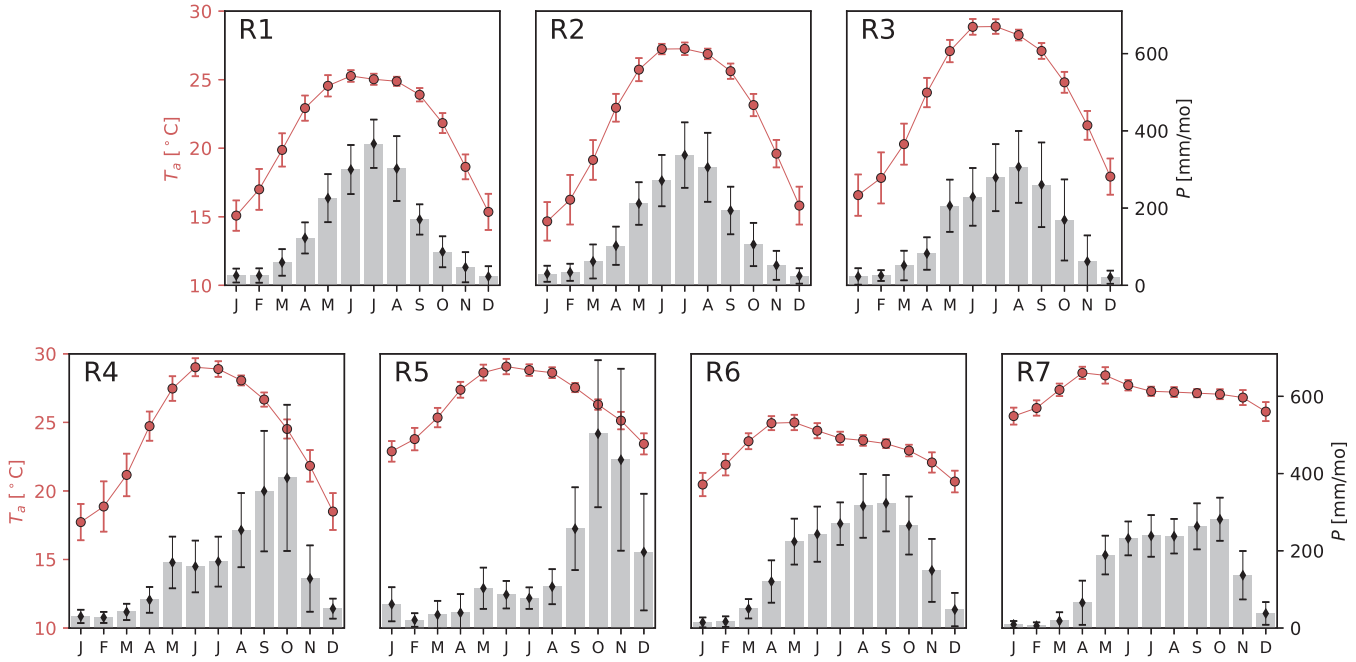

FIGURE 3 Annual cycle of mean air temperature Ta (red lines) and precipitation P (grey bars) over seven climatic sub-regions. Vertical lines represent ± standard deviation [Colour figure can be viewed at wileyonlinelibrary.com]

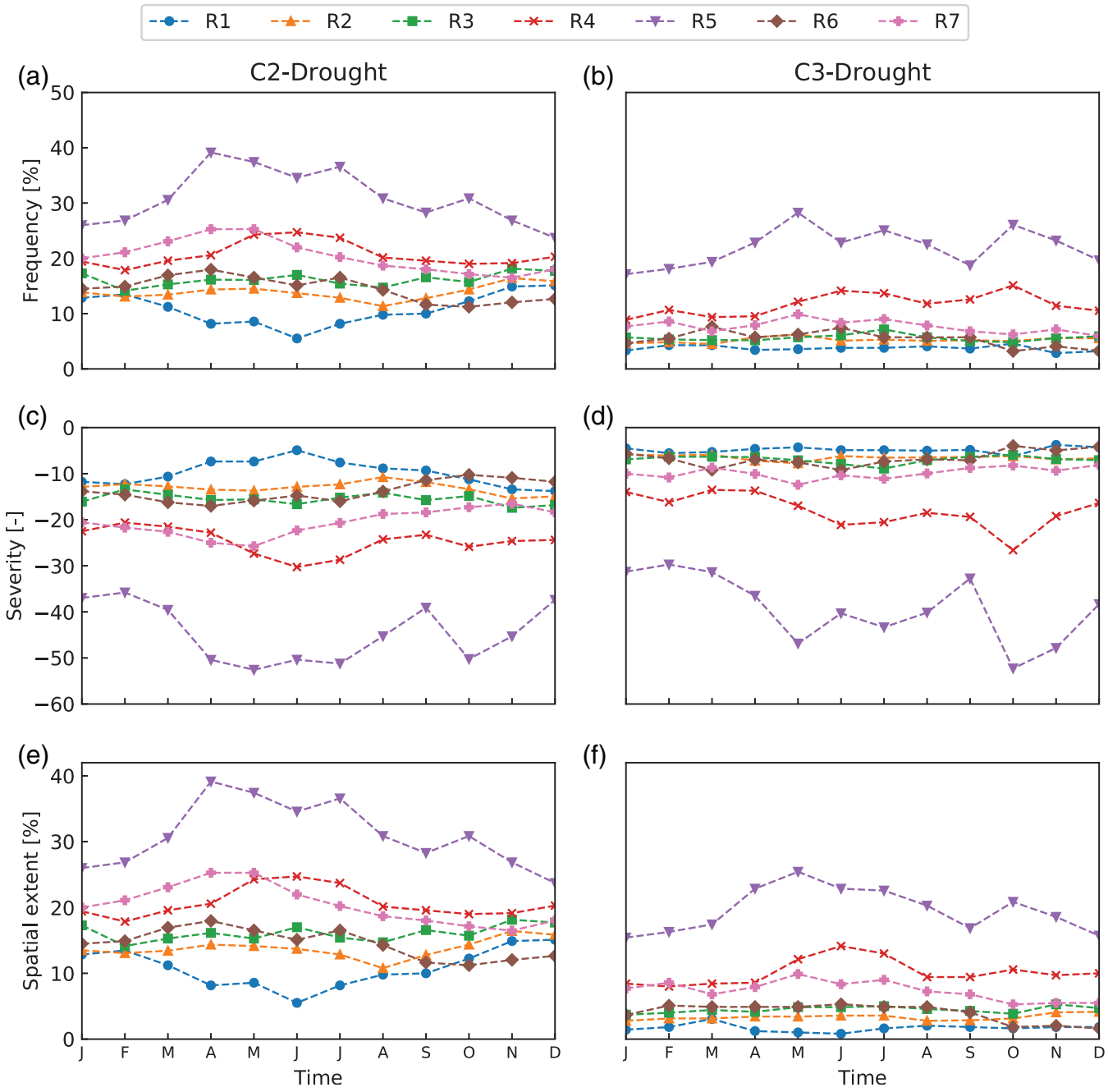

FIGURE 4 Annual cycles of drought characteristics for C2 and C3 levels in seven climatic sub-regions [Colour figure can be viewed at wileyonlinelibrary.com]

smallest values of F, $|S|$, and SE of R1 in C_2 category were found coincident with the peak of temperature during hot summer months (MJJ). Overall, the temporal variability of S and SE were highly correlated with F and there have been sub-regional differences in the temporal variability of these drought characteristics. Moreover, though climate seasonality was observed in many sub-regions, the annual cycles of these two drought characteristics were quite uniform throughout the year, except for R5. The largest values of F, S, and SE found in R5 and R4, especially for C3. This result suggests that the seasonal variability of rainfall and temperature (Figure 3), which controls soil moisture deficit during spring and summer time, could play important roles in the mechanisms and formation of drought in these areas.

3.3 | Spatio-temporal patterns of drought

3.3.1 | Interannual variation of PDSI

Figure 5 suggests a spatial pattern of leading modes of variability in the calculated PDSI. The results indicate that

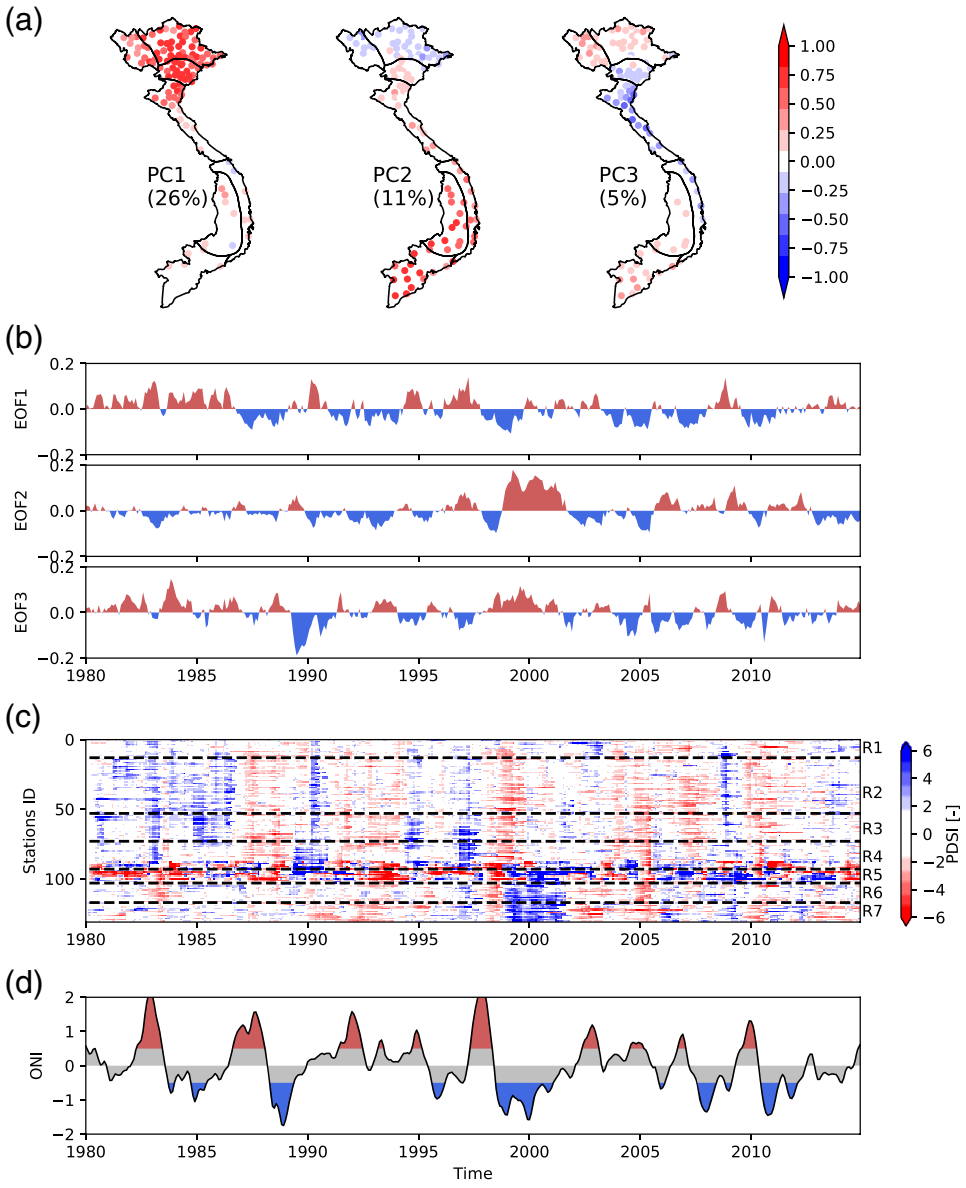

FIGURE 5 Leading modes of variability in PDSI. (a) Patterns of the leading PCs at 131 stations. (b) Principle component time series (EOFs) associated with the leading PCs. (c) Time series of PDSI at 131 stations arranging by sub-regions. (d) Variation of the Oceanic Nino Index (ONI) monthly time series; the grey shade indicates the threshold SST of ±0.5°C that categorizes the ENSO phase as El Niño (red) and La Niña (blue) [Colour figure can be viewed at wileyonlinelibrary.com]

EOF1, EOF2, and EOF3 accounted for 26, 11 and 5% of the total variance, respectively. Collectively, these modes cover the spatial distribution of drought variability over Vietnam. We thus restrict our analysis to these first three PCs. Figure 5a also suggests a regional pattern of PDSI, in which positive (negative) values reflect the positive (negative) correlation between PDSI and different modes. In addition, the variational modes of drought over the Northern (R1-R3) and Southern (R6-R7) regions are similar but they are different to those in the Central region (R4-R5). Particularly, PC1 shows a distinct drought pattern heavily loaded over the Northern region, indicating the largest variability of drought in R1-R3. PC2 reveals a similar pattern of drought variability in R6-R7. This result suggests that the variations of drought in R1-R3 and R6-R7 might be dominated by common factors at the same periods of wet (May to October) and dry (November to April) seasons, respectively. The larger variation of drought in R1-R3 compared to R6-R7 could be attributed to the differences of temperature variability in the Northern area (Figure 3). In contrast, PC3 shows a pattern in which the Central region (R4-R5) exhibits an opposite trend of drought variation. This might be related to the difference of climate conditions in R4-R5 compared to other sub-regions, in which rainy season is shifted to autumn and winter. Moreover, the region usually experiences a hot and dry period in summer caused by the foehn phenomenon at the lee side of Truong Son mountain range during the Southwest Asian monsoon season. The spatial loading of the first three leading modes generally suggests that there are different dominant controls on drought across sub-regions in Vietnam, including both geographical and circulation factors.

The temporal variability of EOFs associated with the leading PCs is shown in Figure 5b. It is observed that

positive (negative) values of EOF1 and EOF2 are associated with positive (negative) values of PDSI in R1-R3 and R6-R7, meanwhile positive (negative) values of EOF3 are linked with negative (positive) values of PDSI in R4-R5 (Figure 5b,c). The opposite signs of EOF1 and EOF2 during some periods suggest that drought events in the Northern and Southern areas are not totally in the same phase. This could be attributed to the differences of large-scale forcing associated with rainfall mechanisms and temperature regimes in these sub-regions (Wang and LI, 2004; Huang *et al*., 2012; Phan *et al.,* 2009, 2018). A similar situation can be observed for EOF3 in comparison to EOF1 and EOF2. Figure 5c shows the variation of C2 drought events detected by PDSI for all stations across climatic sub-regions. The results indicate that, most of drought (wetness) events in R1-R3, northern R4, and R6-R7 are coincident with the periods in which EOF1 and EOF2 are negative (positive). In contrast, drought (wetness) events in R5 and southern R4 correspond to positive (negative) values of EOF3 (Figure 5b). Moreover, the interannual variability of PDSI is in good agreement with the ONI that is often used to identify ENSO events (Figure 5d). For example, El Niño events in 1986–1988, 1991–1992, 1997–1998, etc. (La Niña events in 1988–1989, 1998–2000, etc.) identified by the ONI's values greater (less) than 0.5°C (−0.5°C) are reflected by the corresponding negative (positive) values of EOF1 and EOF2, and positive (negative) values of the EOF3.

3.3.2 | The spatial distributions of drought characteristics

The spatial distributions of four drought characteristics for 131 stations during the 1980–2014 period are shown in Figure 6. The mean duration D_u was generally found larger in the central sub-region (R4-R5) for both C_2 and C_3. This result indicates typically longer periods of drought events in R4-R5. Consequently, frequency F was also found larger there than other sub-regions. In contrast, the inter-arrival time T was quite spatially uniform, suggestive of much shorter non-drought periods in the Central sub-regions (R4-R5). Moreover, severity

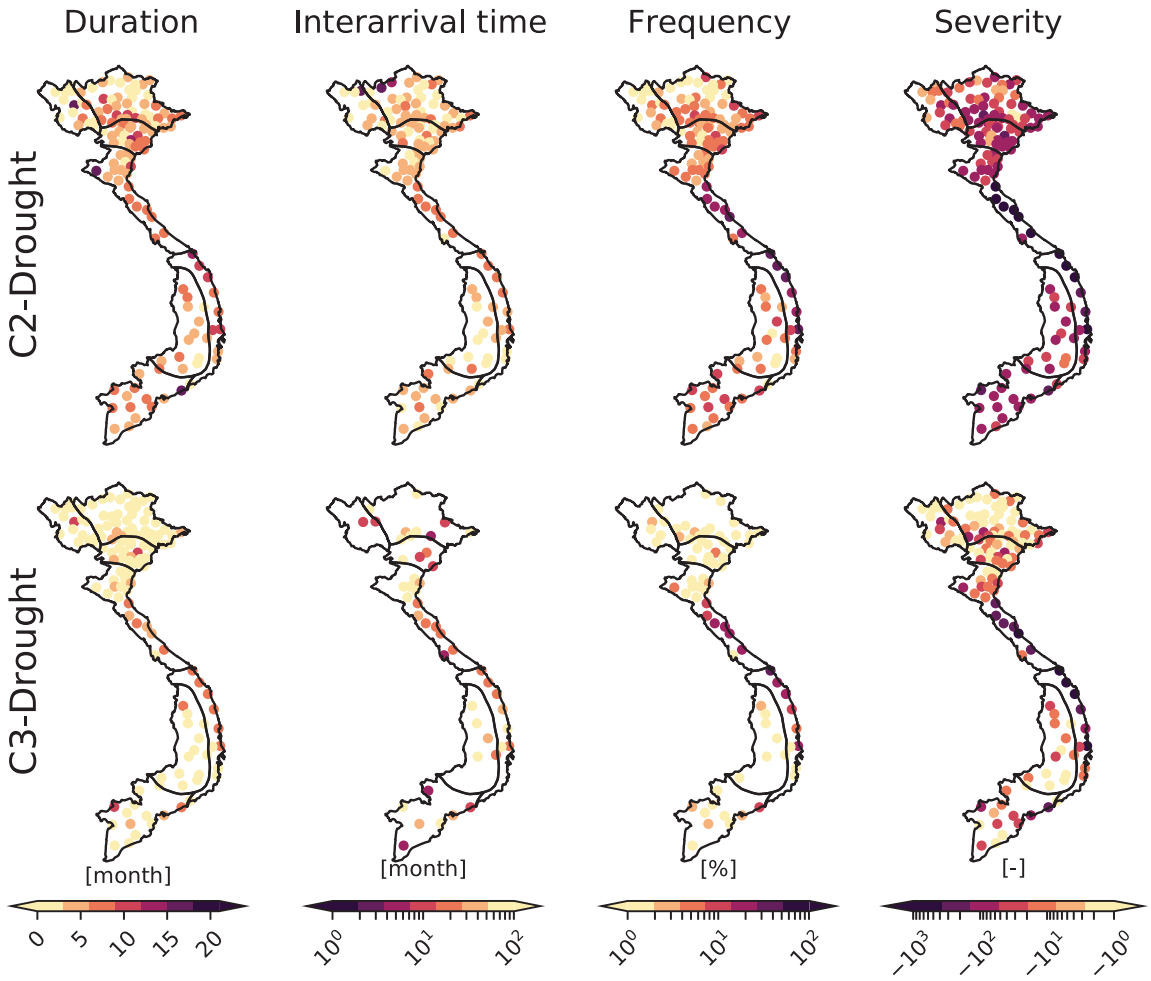

FIGURE 6 Spatial distribution of drought characteristics including mean duration Du, interarrival time T, frequency F, and severity S. Note that the colour bars of T, F, and S are in log-scale [Colour figure can be viewed at wileyonlinelibrary.com]

S was very large in R4-R5, indicating very high intensity of drought events in these sub-regions.

To better examine the regional patterns of drought events, we also identified the sub-regional mean of these four drought characteristics shown above. Figure 7 shows the sub-regional mean of frequency F, severity S, duration D_u, and inter-arrival T for C_2 and C_3 over sub-regions. The results exhibit consistent, regional patterns of these characteristics, except for T in C_2. Here, one should note that F, S, and D_u of C_2 were longer than those of C_3. This is simply because C_3 is a subset of C_2. In addition, the differences between C_2 and C_3 imply the characteristics of moderate drought ($-3 < \text{PDSI} < -2$) in the traditional PDSI classification. While F and S decrease significantly from *C2* to *C3* for most sub-regions, these percentage changes were quite small in R4-R5. This finding confirms that drought in the Central sub-regions is often more severe than in all other areas. Nevertheless, the changes of D_u from C_2 to C_3 in all sub-regions were not as large as other drought characteristics. On average, the variability of D_u was the lowest among all characteristics. In general, the regional patterns of drought characteristics suggest that different sub-regions have different dominant controls on drought, including local climatic and large-scale (see Section 3.5) factors.

3.4 | Trends of drought

The changes in seasonality of drought characteristics also have important impacts on environment. Figure 8 shows the trends of seasonal PDSI variations per decade at 131 stations over the 1980–2014 period. Note that stations with black circles indicate that p-value <.05. Overall, we detected heterogeneity in the historical trends of drought changes across sub-regions during the study period. Specifically, we found a decreasing trend of seasonal PDSI in northern sub-regions (R1-R3), except during summer months (JAS). In contrast, a significant increasing trend of seasonal PDSI was observed in the central coast (R4-R5). In other sub-regions, slightly

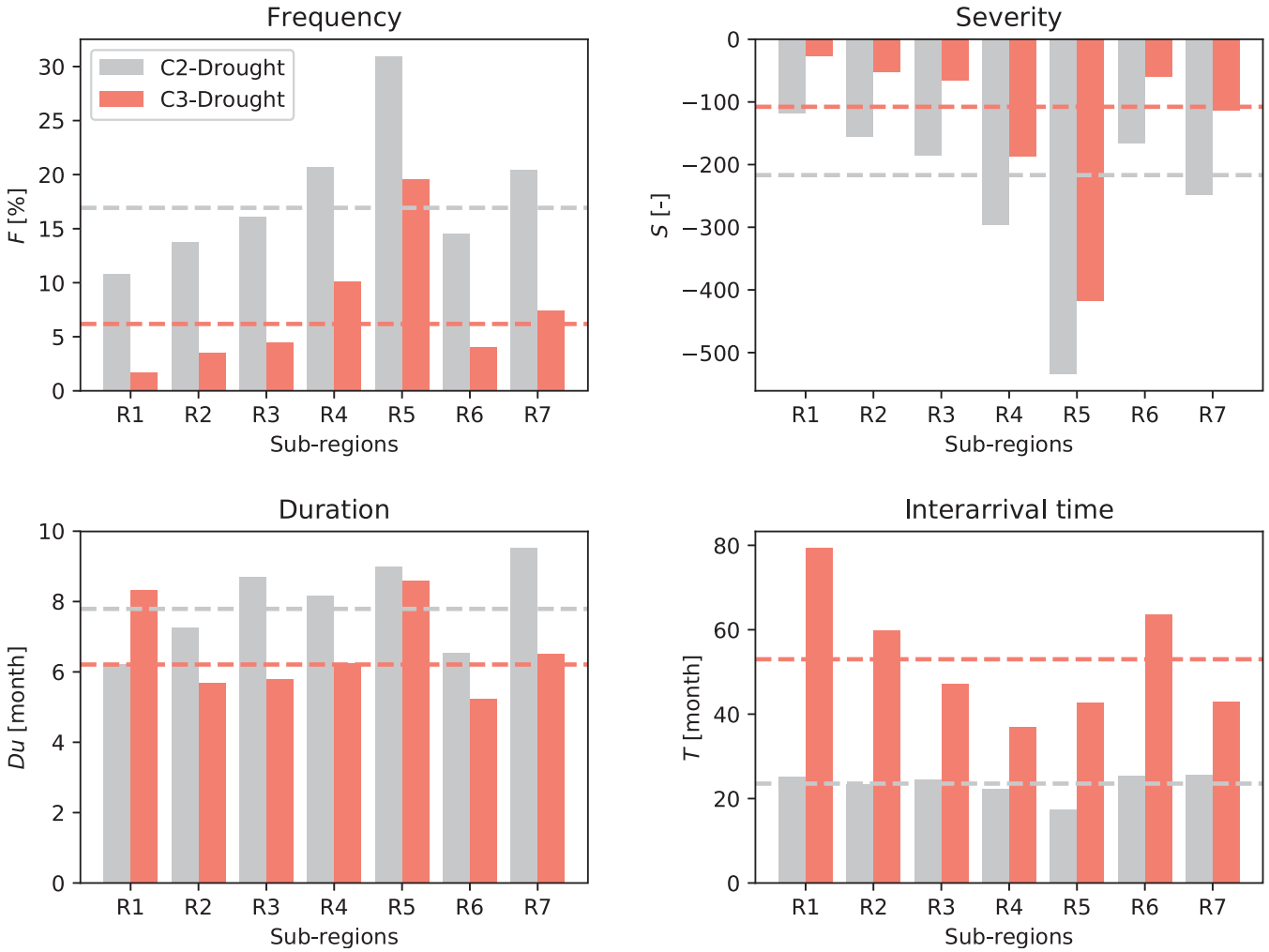

FIGURE 7 Regional mean of drought characteristics for C2 (grey) and C3 (red) over sub-regions. Dash lines represent average values for entire mainland Vietnam [Colour figure can be viewed at wileyonlinelibrary.com]

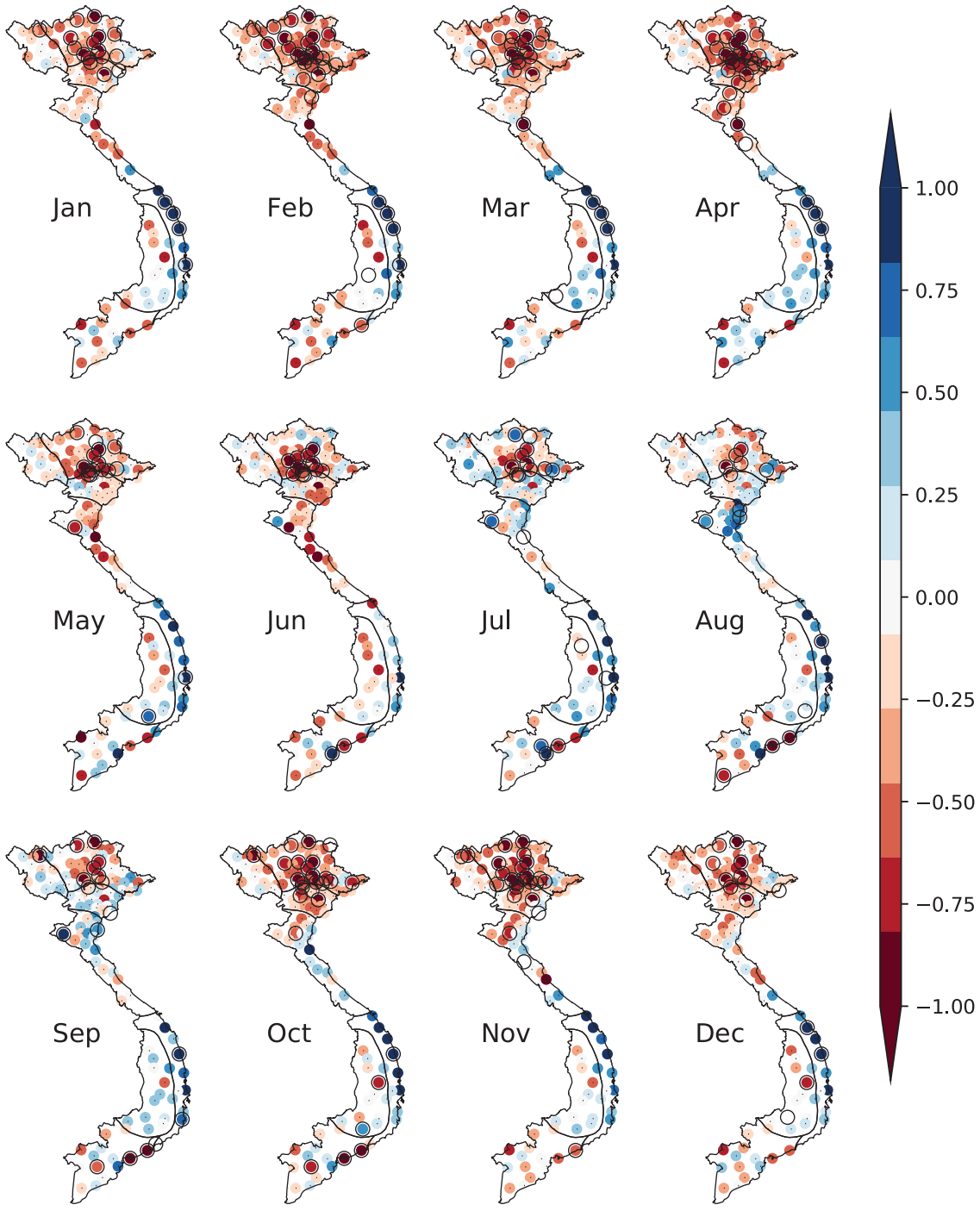

FIGURE 8 Sen's slopes of PDSI per decade calculated for 131 stations during the period 1980–2014. Black circles indicate p-value <.05 [Colour figure can be viewed at wileyonlinelibrary.com]

positive slopes of seasonal PDSI are found, indicating small changes in drought.

3.5 | Linking PDSI and large-scale drivers

How large-scale processes are related to changes in drought in Vietnam remains a question. Here, we examined this relationship by comparing the calculated PDSI time series with the temporal variation of CIs. The correlation coefficients (R) between PDSI at each station and each CI are shown in Figure 9. The results show that PDSI in R6-R7 agrees well with ENSO-related indices (i.e., ONI, SOI, Nino3.4, MEI, RINDO SLPA, CPAC850, REQSOI, WPC850, BEST) with |R| at most stations in the range of

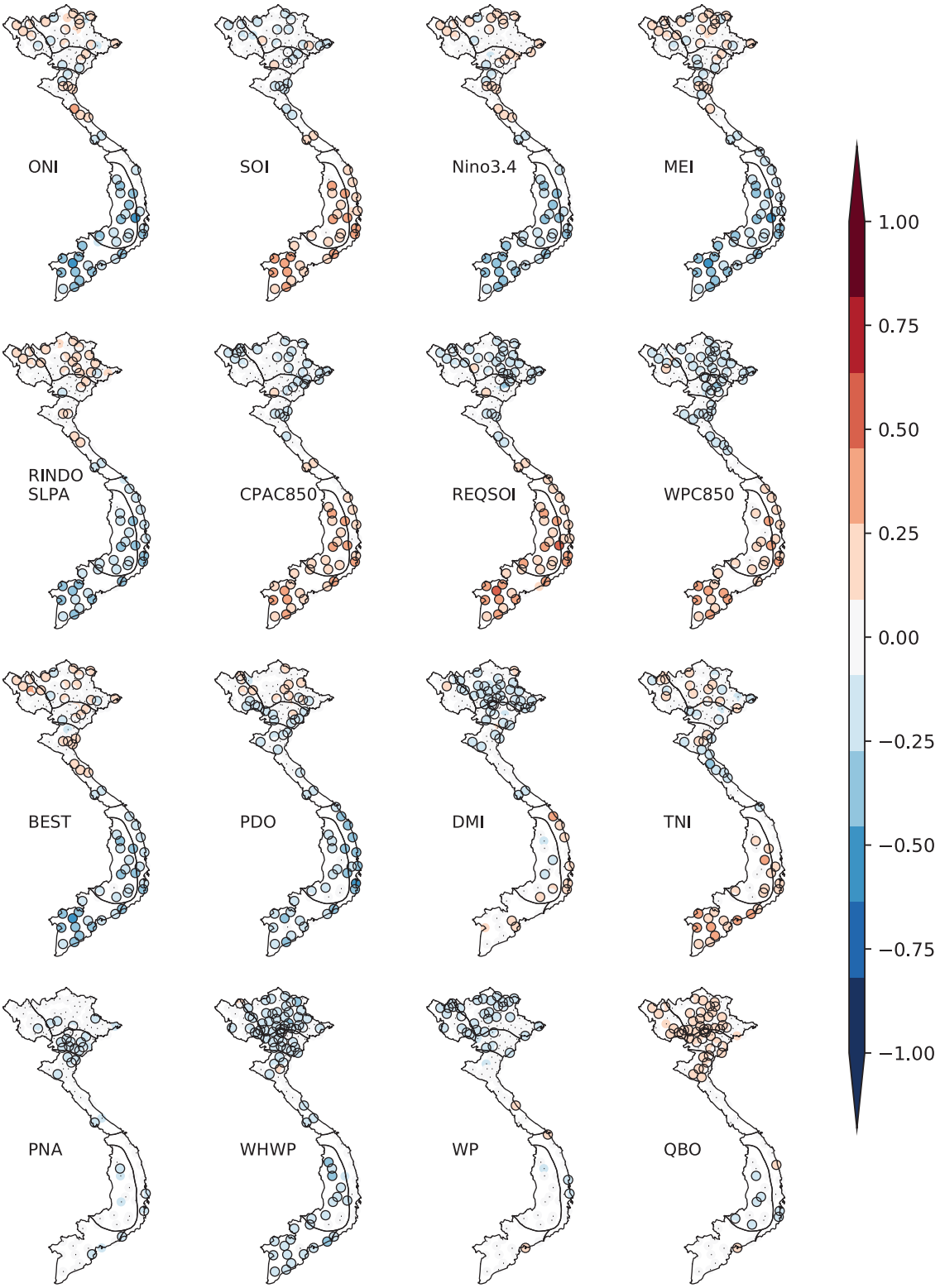

FIGURE 9 Correlation coefficients between PDSI at each station and 16 climate indices. Black circles indicate p-value <.05 [Colour figure can be viewed at wileyonlinelibrary.com]

0.40 ÷ 0.60. Moreover, |R| values in R1-R5 are much smaller and have opposite signs with those in R6-R7. It seems that PDSI in R1-R5 is stronger correlated with PNA, DMI, WHWP, WP, and QBO compared to that in R6-R7. However, these |R| values are quite small (0.10 ÷ 0.20). Furthermore, the R values between regional mean PDSI and

TABLE 3 Correlation coefficients between CIs and (i) sub-regional mean PDSI, (ii) EOFs of PDSI

	(i) Sub-regional mean PDSI							(ii) EOFs of PDSI		
CIs	**R1**	**R2**	**R3**	**R4**	**R5**	**R6**	**R7**	**EOF1**	**EOF2**	**EOF3**
ONI	0.055	0.071	0.032	0.077	**−0.146**	**−0.378**	**−0.437**	0.033	**−0.408**	**−0.201**
SOI	−0.063	−0.053	−0.063	−0.062	**0.204**	**0.303**	**0.343**	−0.043	**0.339**	**0.150**
Nino3.4	0.055	0.041	0.015	0.059	**−0.116**	**−0.327**	**−0.381**	0.013	**−0.350**	**−0.173**
MEI	0.057	0.061	0.020	−0.028	**−0.260**	**−0.399**	**−0.422**	0.013	**−0.442**	−0.088
RINDO_SLPA	0.064	**0.096**	0.059	0.041	**−0.275**	**−0.332**	**−0.333**	0.061	**−0.367**	−0.074
CPAC850	−0.073	**−0.097**	−0.066	−0.048	**0.159**	**0.329**	**0.324**	−0.066	**0.349**	**0.128**
REQSOI	−0.075	**−0.134**	−0.094	−0.042	**0.278**	**0.375**	**0.387**	−0.088	**0.423**	**0.099**
WPC850	−0.039	**−0.149**	**−0.147**	**−0.162**	**0.195**	**0.209**	**0.310**	**−0.133**	**0.277**	**0.188**
BEST	0.075	0.057	0.049	0.079	**−0.195**	**−0.331**	**−0.401**	0.039	**−0.375**	**−0.176**
PDO	−0.033	0.030	−0.058	**−0.142**	**−0.500**	**−0.231**	**−0.250**	−0.047	**−0.333**	**0.134**
DMI	−0.011	**−0.165**	**−0.120**	−0.095	**0.211**	−0.020	0.078	**−0.131**	0.077	0.010
TNI	−0.011	0.023	0.019	**−0.150**	0.054	**0.139**	**0.368**	0.026	**0.215**	**0.295**
PNA	−0.041	−0.081	**−0.125**	**−0.101**	**−0.118**	−0.061	−0.070	**−0.108**	−0.084	0.065
WHWP	**−0.109**	**−0.229**	**−0.201**	**−0.147**	−0.059	**−0.247**	**−0.262**	**−0.236**	**−0.214**	**−0.124**
WP	**−0.170**	**−0.140**	−0.078	0.023	0.016	0.017	0.030	**−0.123**	0.056	**−0.099**
QBO	**0.180**	**0.126**	0.094	0.045	0.021	−0.063	0.022	**0.140**	−0.053	0.044

Bold text implies values satisfy the significance level of .05 for a two-sided *t* test.

each CI are presented in Table 3, indicating that drought in R1-R4 has almost no correlation with CIs reflected by small values of |R| (0.20 ÷ 0.22). Compared to all other sub-regions, the Central Highland (R6) and Southern (R7) sub-regions show quite significant correlations between PDSI and ENSO-related CIs, with |R| (between regional mean PDSI and CIs) mostly ranging from 0.33 ÷ 0.40. However, the correlations between PDSI and DMI, and other indices such as WP, QBO, PNA, are low. Table 3 further shows the R values between the CIs and EOFs of the PDSI. The results imply a good correlation between EOF2, associated with drought pattern in R6-R7, and ENSO-related CIs with |R| values mostly range from 0.33 to 0.45. In contrast, EOF3 associated with drought in R1-R3 has no correlation with the ENSO-related CIs, it rather seems to be correlated with other CIs such as PNA, DMI, WHWP, WP and QBO. However, the |R| values are quite small (∼ 0.1 ÷ 0.2). This discrepancy is attributed to the different influences of large-scale factors on the rainfall and temperature regimes over these sub-regions. Despite similar patterns of drought variability, rainfall and temperature in R6-R7 is dominated by the Asian summer monsoon which is strongly associated with ENSO activities (Ju and Slingo, 1995; Kinter *et al.,* 2002; Yan *et al.,* 2018), meanwhile rainfall in R1-R3 is mainly driven by the Intertropical Conversion Zone (ITCZ) and/or tropical cyclone activities (Nguyen-Thi *et al.,* 2012). Moreover, unlike R6-R7, temperature regime in R1-R3 is strongly associated with the penetration of cold surges during winter time that may cause substantail drops in air temperature at some areas. The correlation between EOF3, associated with drought pattern in R4-R5, and ENSO-related CIs is quite similar, but |R| values are much smaller compared to those of EOF2.

PCA analysis for the CIs shows that the first three modes contributed 65% of the total variance, including ENSO-related indices (PC1, 48%), DMI, TNI, PNA, and WHWP indices (PC2, 9%), and PDO, WP, and QBO indices (PC3, 8%), respectively (not show). The correlation coefficients between time series of the PCs (also denoted by EOFs) of the CIs and EOFs of PDSI are shown in Table 4. The results show that the PDSI's EOF2 correlates quite well with CI's EOF1, indicating that drought in the R6-R7 is strongly

TABLE 4 Correlation coefficients between principle components of PDSIs and CIs

	PDSIs		
CIs	**PDSI_EOF1**	**PDSI_EOF2**	**PDSI_EOF3**
CI_EOF1	0.032	**−0.433**	**−0.152**
CI_EOF2	**−0.237**	0.074	0.09
CI_EOF3	−0.004	**−0.159**	**0.213**

Bold text implies values satisfy the significance level of .05 for a two-sided *t* test.

associated with ENSO events (CI's EOF1) and somewhat with PDO, WP, and QBO (CI's EOF3). While drought in R1-R3 and northern R4 is partly influenced by the variability of DMI, TNI, PNA, and WHWP (CI's EOF2), drought in the R5 and southern R4 is weakly associated with both CI's EOF1 and CI's EOF3. In general, the obtained results here are consistent with those mentioned above.

4 | CONCLUSIONS

In this study, we used the Palmer Drought Severity Index (PDSI) to analyse the space–time variability of drought over the mainland Vietnam for the 1980–2014 period. We applied PCA and statistical tests to analyse the dominant variability and long-term trends of droughts, and their teleconnections with large-scale atmospheric and ocean processes. To the best of our knowledge, this study is the first in the literature that uses PDSI to examine the spatio-temporal variability of drought characteristics over Vietnam. This multivariate approach offers a more realistic assessment of droughts across climate sub-regions, especially under the context of anthropogenic global warming that has occurred since the 20th century.

Unlike other drought indices used in previous studies in Vietnam, PDSI incorporates prior precipitation, moisture supply, runoff and evaporation demand at the surface level, which reveals new insights of drought pattern in Vietnam. We show that drought characteristics vary quite significantly among sub-regions, exhibiting apparent seasonal variations and regional patterns. For example, the largest frequency, intensity, and severity of drought are often observed in the Central area (R4-R5). This could be partially attributed to soil moisture deficit associated with low rainfall and high temperature during summer. Moreover, our results suggest different trends of drought evolution over sub-regions. While predominantly decreasing (increasing) trends are found in the Northern (North Central) sub-regions, changes in drought in the Southern area are relatively small. Another key finding is that the linkages between drought in Vietnam and large-scale drivers are quite different among climatic sub-regions. While droughts in R6-R7 sub-regions are linked more strongly with ENSO events, droughts in the remaining sub-regions are partly influenced by the variability of the other teleconnection patterns such as DMI, TNI, etc.

The spatial dynamics of PDSI revealed three major patterns of droughts. The first one showed a distinct drought pattern loaded over the north sub-regions (R1-R3), indicating the largest variability of drought here. The second pattern indicated opposite variations of droughts between the Northern (R1-R3) and the Southern (R6-R7) sub-regions. Finally, the third one suggested that droughts in the Central sub-regions (R4-R5) was further controlled by local factors, that is, the foehn effect because the sub-regions are located on the lee side of a mountain range. These three leading modes together explain 43% of the drought variability in Vietnam and imply a combined effects of factors that control drought over Vietnam, including climate seasonality, large-scale drivers, and landscape conditions. The results also indicated that drought variability in the South Central (R5) and Southern (R6-R7) sub-regions has been highly sensitive to ENSO, suggesting a possibility of early prediction for drought in these sub-regions.

We believe that the results obtained in this study is an important step forward to improve the management of drought impacts in Vietnam, including the local and regional societal impacts, water resources, agriculture, and the ecosystem response. The PDSI analysis showed high correlations with rainfall and air temperature across Vietnam but the possibility to combined PDSI with other drought indices to better represent extreme rainfall and dry conditions in the region could be explored in future work. Further research should also be directed toward better understanding the long-term drivers of drought variability and its propagation to other types of drought.

ACKNOWLEDGEMENTS

This research is supported by the National Project under grant number KC.09.15/16-20. P.V.V.L. was supported by Vietnam National Foundation for Science and Technology Development (NAFOSTED) under grant number 105.06-2017.320. Two journal reviewers provided excellent comments to improve the quality of the manuscript.

ORCID

Phong V. V. Le https://orcid.org/0000-0001-5558-1023
Tan Phan-Van https://orcid.org/0000-0003-0756-1217

REFERENCES

Abdi, H. and Williams, L.J. (2010) Principal component analysis. *Wiley Interdisciplinary Reviews: Computational Statistics*, 2, 433–459.

Aghakouchak, A. (2015) Recognize anthropogenic drought. *Nature*, 524, 409–411.

Aghakouchak, A., Cheng, L., Mazdiyasni, O. and Farahmand, A. (2014) Global warming and changes in risk of concurrent climate extremes: insights from the 2014 California drought. *Geophysical Research Letters*, 41, 8847–8852.

Alley, W.M. (1984) The Palmer drought severity index: limitations and assumptions. *Journal of Climate and Applied Meteorology*, 23, 1100–1109.

AMS. (2004) Statement on meteorological drought. *Bulletin of the American Meteorological Society*, 85, 771–773.

Cook, B.I., Ault, T.R. and Smerdon, J.E. (2015) Unprecedented 21st century drought risk in the American Southwest and Central Plains. *Science Advances*, 1, e1400082.

CPC. 2011. *Monthly Atmospheric and SST Indices*. NOAA/National Weather Service, MD [Online].

Dai, A. (2010) Characteristics and trends in various forms of the Palmer drought severity index during 1900–2008. *Journal of Geophysical Research: Atmospheres*, 116, 1–26.

Dai, A., Trenberth, K.E. and Qian, T. (2004) A global dataset of Palmer drought severity index for 1870–2002: relationship with soil moisture and effects of surface warming. *Journal of Hydrometeorology*, 5, 1117–1130.

Dracup, J.A., Lee, K.S. and Paulson, E.G. (1980) On the definition of droughts. *Water Resources Research*, 16, 297–302.

ESRL-PSD. 2018. *Climate Indices: Monthly Atmospheric and Ocean Time Series*. NOAA, CO [Online].

FAO/IIASA/ISRIC/ISS-CAS/JRC. (2009) *Harmonized World Soil Database (version 1.1)*. Rome, Italy: FAO.

Ge, Y., Apurv, T. and Cai, X. (2016) Spatial and temporal patterns of drought in the continental U.S. during the past century. *Geophysical Research Letters*, 43, 6294–6303.

Gocic, M. and Trajkovic, S. (2014) Analysis of trends in reference evapotranspiration data in a humid climate. *Hydrological Sciences Journal*, 59, 165–180.

Qian, H. and Yuping, G. (2012) Does the Asian monsoon modulate tropical cyclone activity over the South China Sea? *Chinese Journal of Oceanology and Limnology*, 30, 960–965. https://doi.org/10.1007/s00343-012-1273-x.

Ju, J. and Slingo, J. (1995) The Asian summer monsoon and ENSO. *Quarterly Journal of the Royal Meteorological Society*, 121, 1133–1168.

Karl, T.R. (1986) The sensitivity of the Palmer drought severity index and Palmer's Z-index to their calibration coefficients including potential evapotranspiration. *Journal of Climate and Applied Meteorology*, 25, 77–86.

Kendall, M. G. 1955. *Rank Correlation Methods*, 2nd edition. London: Charles Griffin & Co.

Kinter, J.L., Miyakoda, K. and Yang, S. (2002) Recent change in the connection from the Asian monsoon to ENSO. *Journal of Climate*, 15, 1203–1215.

Le, M.H., Perez, G.C., Solomatine, D. and Nguyen, L.B. (2016) Meteorological drought forecasting based on climate signals using artificial neural network – a case study in Khanhhoa Province Vietnam. *Procedia Engineering*, 154, 1169–1175.

Lever, J., Krzywinski, M. and Altman, N. (2017) Principal component analysis. *Nature Methods*, 14, 641–642.

Li, Z., Chen, Y., Fang, G. and Li, Y. (2017) Multivariate assessment and attribution of droughts in Central Asia. *Scientific Reports*, 7, 1316.

Lima, C.H.R. and Aghakouchak, A. (2017) Droughts in Amazonia: spatiotemporal variability, teleconnections, and seasonal predictions. *Water Resources Research*, 53, 10824–10840.

Lloyd-Hughes, B. and Saunders, M.A. (2002) A drought climatology for Europe. *International Journal of Climatology*, 22, 1571–1592.

van Loon, A.F. (2015) Hydrological drought explained. *Wiley Interdisciplinary Reviews: Water*, 2, 359–392.

Mai, V.K., Grace, R., Carol, M. and Tran, T. (2014) Evaluation of dynamically downscaled ensemble climate simulations for Vietnam. *International Journal of Climatology*, 34, 2450–2463.

Mann, H.B. (1945) Nonparametric tests against trend. *Econometrica: Journal of the Econometric Society*, 13, 245–259.

Mishra, A.K. and Singh, V.P. (2010) A review of drought concepts. *Journal of Hydrology*, 391, 202–216.

Nguyen-Thi, H.A., Matsumoto, J., Ngo-Duc, T. and Endo, N.J.S. (2012) A climatological study of tropical cyclone rainfall in Vietnam. *SOLA*, 8, 41–44.

Palmer, W.C. (1965) *Meteorological Drought*. Washington, DC: U.S. Weather Bureau, Research Paper Number 45, p. 58.

Phan, V.-T., Ngo-Duc, T. and Ho, T.-M.-H. (2009) Seasonal and interannual variations of surface climate elements over Vietnam. *Climate Research*, 40, 49–60.

Phan, V.T., Nguyen-Xuan, T., Van Nguyen, H., Laux, P., Ha, P.-T. and Ngo-Duc, T. (2018) Evaluation of the NCEP climate forecast system and it's downscaling for seasonal rainfall prediction over Vietnam. *Weather and Forecasting*, 33, 615–640. https://doi.org/10.1175/WAF-D-17-0098.1.

Ringnér, M. (2008) What is principal component analysis? *Nature Biotechnology*, 26, 303–304.

Rippey, B.R. (2015) The U.S. drought of 2012. *Weather and Climate Extremes*, 10, 57–64.

Saghafian, B. and Mehdikhani, H. (2014) Drought characterization using a new copula-based trivariate approach. *Natural Hazards*, 72, 1391–1407.

van der Schrier, G., Briffa, K.R., Jones, P.D. and Osborn, T.J. (2006) Summer moisture variability across Europe. *Journal of Climate*, 19, 2818–2834.

Schwalm, C.R., Anderegg, W.R.L., Michalak, A.M., Fisher, J.B., Biondi, F., Koch, G., Litvak, M., Ogle, K., Shaw, J.D., Wolf, A., Huntzinger, D.N., Schaefer, K., Cook, R., Wei, Y., Fang, Y., Hayes, D., Huang, M., Jain, A. and Tian, H. (2017) Global patterns of drought recovery. *Nature*, 548, 202.

Sen, P.K. (1968) Estimates of the regression coefficient based on Kendall's tau. *Journal of the American Statistical Association*, 63, 1379–1389.

Sheffield, J., Wood, E.F. and Roderick, M.L. (2012) Little change in global drought over the past 60 years. *Nature*, 491, 435–438.

Shukla, S., Safeeq, M., Aghakouchak, A., Guan, K. and Funk, C. (2015) Temperature impacts on the water year 2014 drought in California. *Geophysical Research Letters*, 42, 4384–4393.

Thornthwaite, C.W. and Mather, J.R. (1955) *The Water Balance*. Centerton, NJ: Drexel Institute of Technology, Laboratory of Climatology.

Tran, T. (2012) Study on droughts in the south central and the central highlands. *VNU Journal of Science: Earth and Environmental Sciences*, 28, 125–132.

Vu, T. and Mishra, A. (2016) Spatial and temporal variability of standardized precipitation index over Indochina peninsula. *Cuadernos de Investigacion Geografica*, 42, 221–232.

Vu, M.T., Raghavan, S.V., Pham, D.M. and Liong, S.-Y. (2015) Investigating drought over the Central Highland, Vietnam, using regional climate models. *Journal of Hydrology*, 526, 265–273.

Vu, T.M., Raghavan, S.V., Liong, S.-Y. and Mishra, A.K. (2017) Uncertainties of gridded precipitation observations in characterizing spatio-temporal drought and wetness over Vietnam. *International Journal of Climatology*, 38, 2067–2081.

Vu-Thanh, H., Ngo-Duc, T. and Phan-Van, T. (2014) Evolution of meteorological drought characteristics in Vietnam during the 1961-2007 period. *Theoretical and Applied Climatology*, 118, 367–375.

Wang, B. and LI, T. (2004) East Asian monsoon and ENSO interaction. In: Chang, C.P. (Ed.) *East Asian Monsoon*. Hackensack, NJ: World Science, p. 177, 212.

Wells, N., Goddard, S. and Hayes, M.J. (2004) A self-calibrating Palmer drought severity index. *Journal of Climate*, 17, 2335–2351.

Wilhite, D. (2000) Drought as a natural hazard: concepts and definitions. In: *Drought, A Global Assessment*. London, UK: Routledge, pp. 3–18.

Wilhite, D.A. and Glantz, M.H. (1985) Understanding: the drought phenomenon: the role of definitions. *Water International*, 10, 111–120.

WMO 2006. *Drought Monitoring and Early Warning: concepts, Progress and Future Challenges*. Collection(s) and Series: WMO- No. 1006. ISBN: 978-92-63-11006-0.

Xukai, Z., Panmao, Z. and Qiang, Z. (2005) Variations in droughts over China: 1951–2003. *Geophysical Research Letters*, 32, 1–4. https://doi.org/10.1029/2004GL021853.

Yan, X., Konopka, P., Ploeger, F., Tao, M., Müller, R., Santee, M.L., Bian, J. and Riese, M. (2018) El Niño southern oscillation influence on the Asian summer monsoon anticyclone. *Atmospheric Chemistry and Physics*, 18, 8079–8096.

Zargar, A., Sadiq, R., Naser, B. and Khan, F.I. (2011) A review of drought indices. *Environmental Reviews*, 19, 333–349.

How to cite this article: Le PVV, Phan-Van T, Mai KV, Tran DQ. Space–time variability of drought over Vietnam. *Int J Climatol*. 2019;39:5437–5451. https://doi.org/10.1002/joc.6164